

# UC Berkeley

## UC Berkeley Previously Published Works

### Title

Ultrahigh thermal conductivity of isotopically enriched silicon

### Permalink

<https://escholarship.org/uc/item/7rb822x7>

### Journal

Journal of Applied Physics, 123(9)

### ISSN

0021-8979

### Authors

Inyushkin, Alexander V  
Taldenkov, Alexander N  
Ager, Joel W  
[et al.](#)

### Publication Date

2018-03-07

### DOI

10.1063/1.5017778

Peer reviewed

# Extra-high thermal conductivity of isotopically enriched silicon

Alexander V. Inyushkin\* and Alexander N. Taldenkov<sup>†</sup>

*National Research Center Kurchatov Institute, Moscow 123182, Russia*

Joel Ager, III<sup>‡</sup> and Eugene E. Haller<sup>§</sup>

*Materials Sciences Division,*

*Lawrence Berkeley National Laboratory,*

*Berkeley, California 94720 and*

*Department of Materials Science and Engineering,*

*University of California at Berkeley, Berkeley, California 94720*

Helge Riemann<sup>¶</sup> and Nikolay V. Abrosimov<sup>\*\*</sup>

*Leibniz-Institut für Kristallzüchtung, 12489 Berlin, Germany*

Hans-Joachim Pohl<sup>††</sup>

*VITCON Projectconsult GmbH, 07745 Jena, Germany*

Peter Becker<sup>‡‡</sup>

*Physikalisch-Technische Bundesanstalt,*

*Bundesallee 100, 38116 Braunschweig, Germany*

(Dated: November 22, 2017)

## Abstract

Most of stable elements (about eighty) have two and more stable (non-radioactive) isotopes. The physical properties of materials composed of such elements depend on the isotopic abundance in some extent. Remarkably strong isotope effect is observed in the phonon thermal conductivity, the principal mechanism of heat conduction in nonmetallic crystals. An isotopic disorder due to random distribution of the isotopes in the crystal lattice sites results in a rather strong phonon scattering and, consequently, in a reduction of thermal conductivity. In this paper we present new results of accurate and precise measurements of thermal conductivity  $\kappa(T)$  for silicon single crystals having three different isotopic compositions at temperatures  $T$  from 2.4 to 420 K. The highly enriched crystal containing 99.995% of  $^{28}\text{Si}$ , which is one of the most perfect crystal ever synthesized, demonstrates the thermal conductivity about  $450 \text{ W cm}^{-1} \text{ K}^{-1}$  at 24 K, the highest measured value among bulk dielectrics, which is *ten times* greater than one for its counterpart  $^{\text{nat}}\text{Si}$  with the natural isotopic constitution. For highly enriched crystal  $^{28}\text{Si}$  and crystal  $^{\text{nat}}\text{Si}$  the measurements were performed for two orientations [001] and [011], a magnitude of the phonon focusing effect on thermal conductivity was determined accurately at low temperatures. The  $\kappa(T)$  measured in this work gives the most accurate approximation of the intrinsic thermal conductivity of single crystal silicon which is determined solely by the anharmonic phonon processes and diffusive boundary scattering over a wide temperature range.

PACS numbers: 66.70.Df, 63.20.kp, 63.20.kg

---

\* Inyushkin'AV@nrcki.ru

† Taldenkov'AN@nrcki.ru

‡ jwager@lbl.gov

§ eehaller@lbl.gov

¶ helge.riemann@ikz-berlin.de

\*\* nikolay.abrosimov@ikz-berlin.de

†† pohl.vitcon@t-online.de

‡‡ peter.becker@ptb.de

*Keywords:* Silicon, Thermal conductivity, Phonon-defect interaction, Phonon-phonon interaction, Isotope effect

## I. INTRODUCTION

In a number of semiconductor crystals with natural isotopic compositions of elements, the thermal resistivity due to isotope scattering of phonons adds sizably to the total resistivity at room temperature, and may dominate strongly over others at low temperatures (see, e.g., surveys in [1, 2]). Experimental studies showed that the isotope effect on thermal conductivity for crystals with natural isotopic abundances amounts to 50% for diamond [3–6], 20% for germanium [7, 8], about 10% for silicon [9–11], and 5% for GaAs [12] at room temperature. In chemically pure and defect-free crystals, the magnitude of the isotope effect depends on the rates of isotope scattering and anharmonic phonon-phonon scattering, the latter are intrinsic scattering processes which govern thermal conductivity at high temperatures.

The phonon scattering induced by isotopic disorder in crystal lattice is a relatively simple phenomena, and its scattering rate can be calculated reliably in many cases, especially for the normal (‘non-quantum’) crystals [13–15]. For this reason the experimental data on the isotope effect in thermal conductivity is used commonly to validate different theoretical models of heat conduction in crystals. They include various modifications of the Callaway theory [16] based on the Boltzmann transport equation and formulated within a single-mode relaxation time approximation [5, 8, 16–19], new *ab initio* Boltzmann transport approaches [20–25]. In theoretical calculations the estimation of the phonon-phonon scattering processes is an especially challenging task (see, for example, Refs. [23, 26–28]). In this respect, experimental data on thermal conductivity of single-isotope crystal are the most valuable since they represent almost solely the phonon-phonon processes over a wide temperature range.

The most accurate measurements of thermal conductivity for isotopically modified single crystal silicon have been performed in Refs. [9, 11]. The isotopic enrichment of the crystal studied in Ref. [9] was low, 99.896%  $^{28}\text{Si}$ , and the temperature interval of measurements was restricted within 80–300 K. In Ref. [11] the enrichment was higher, 99.983%  $^{28}\text{Si}$  and  $\kappa(T)$  was measured in a much wider temperature range from 0.5 to 300 K. The coincidence of the data for  $^{28}\text{Si}$  and  $^{\text{nat}}\text{Si}$  at low temperatures proved the consistency of the data obtained in that work [11].

In this paper we report on thermal conductivity measurements of silicon single crystals with three different isotopic compositions and orientations including the most perfect nowadays single crystal silicon highly enriched up to 99.995% with the isotope  $^{28}\text{Si}$ . In this unique crystal, grown under the Avogadro project [29], the isotopic scattering rate of phonon is reduced by 4 times as compare with that in enriched crystal  $^{28}\text{Si}$  studied in Ref. [11] and by 2500 times lower than in the crystal with natural isotopic abundance. The prime goals of this work were the accurate and precise determination of the *intrinsic* thermal conductivity of silicon in a wide temperature range and the magnitude of phonon focusing effect in thermal conductivity.

## II. MATERIALS AND METHODS

Single crystals of silicon with different isotopic composition were grown by the floating zone process in Institute of Crystal Growth (IKZ, Berlin, Germany). The silicon boules were dislocation free. Concentrations of electrically active impurities P and B were approximately  $5 \times 10^{15} \text{ cm}^{-3}$  and  $2 \times 10^{14} \text{ cm}^{-3}$ , respectively, and of carbon and substitutional oxygen were  $< 1 \times 10^{16} \text{ cm}^{-3}$  and  $1.6 \times 10^{14} \text{ cm}^{-3}$ , respectively, in the crystal  $^{28}\text{SiB}$  (see Ref. [30] for details). The crystal  $^{28}\text{SiA}$  was cut from the parent crystalline boule number Si28-10Pr11 grown within the Avogadro project in 2007 [29, 31]. It had the concentration of carbon of  $< 1 \times 10^{15} \text{ cm}^{-3}$ , of oxygen of  $\lesssim 4 \times 10^{14} \text{ cm}^{-3}$ , of all others impurities of  $< 1 \times 10^{14} \text{ cm}^{-3}$ , and of vacancies of  $\sim 3 \times 10^{14} \text{ cm}^{-3}$ . The isotopic parameters of these crystals are listed in Table I. The dimensionless parameter

$$g_2 = \sum_i f_i (\Delta M_i / M)^2 \quad (1)$$

characterizes the isotopic disorder. Here  $f_i$  is the concentration of the  $i$ -th isotope, whose mass  $M_i$  differs from the average mass  $M = \sum_i f_i M_i$  by  $\Delta M_i = M_i - M$ .

Rectangular silicon rods were cut from the ingots using a diamond saw. These rods had approximately  $4.35 \times 4.35 \text{ mm}^2$  cross-section and length of about 40.0 mm. The rods were subjected to hand lapping with an abrasive powder suspended in a water. The powder grit size of  $40 \text{ }\mu\text{m}$  was used to lapping all rods surfaces to side dimension of 4.10 mm. The final lapping was performed with  $14 \text{ }\mu\text{m}$  grit abrasive powder. The average surface roughness amplitude  $R_a$  was measured to be 0.20–0.25  $\mu\text{m}$ . Note that the sub-surface damage layer

TABLE I. Characteristics of crystals.  $\Delta N = |N_d - N_a|$ , is the net concentration of the electrically active impurities as estimated from the electrical resistivity at room temperature.

Crystal	$^{28}\text{Si}$	$^{29}\text{Si}$	$^{30}\text{Si}$	$g_2$	type	$\rho$	$\Delta N$
	%	%	%	$10^{-6}$		$\Omega \text{ cm}$	$10^{12} \text{ cm}^{-3}$
$^{\text{nat}}\text{SiA}$	92.223	4.685	3.092	200.7	$p$	2340	5.5
$^{\text{nat}}\text{SiB}$	92.223	4.685	3.092	200.7	$n$	1010	4.3
$^{28}\text{SiA}$	99.995	0.0046	0.0004	0.08	$p$	1020	13
$^{28}\text{SiB}$	99.92	0.07	0.01	1.40	$n$	7.4	600

with the strongly modified properties of silicon is estimated to be about as thick as the abrasive grit size used [32]. The final side dimensions of the samples were  $4.00 \pm 0.005$  mm. The isotopic composition, orientation and dimensions of the samples are given in Table II.

TABLE II. Sample characteristics.  $L$  is the total sample length,  $L_T$  is the distance between two thermometers attached to a sample. Absolute error is 0.1 mm in the sample length, the value of  $L_T$  is known within 0.2–0.3 mm uncertainty.

Sample	$^{28}\text{Si}$	Axis	$L$	$L_T$	$T_{\text{max}}$	$\kappa_{\text{max}}$
	%		mm	mm	K	$\text{W cm}^{-1}\text{K}^{-1}$
$^{\text{nat}}\text{SiA100}$	92.223	[100]	40.0	27.3	22.3	45.5
$^{\text{nat}}\text{SiA110}$	92.223	[110]	40.0	28.2	23.9	43.8
$^{\text{nat}}\text{SiB100}$	92.223	[100]	39.5	26.8	22.3	45.7
$^{28}\text{SiA100}$	99.995	[100]	38.5	26.7	24.1	451
$^{28}\text{SiA110}$	99.995	[110]	40.2	26.3	25.3	420
$^{28}\text{SiB100}$	99.92	[100]	39.5	27.7	24.5	280

Thermal conductivity was measured by the steady-state heat flow technique with two thermometers and one heater. A thick film resistor with  $6.3 \times 3.2 \times 0.55 \text{ mm}^3$  dimensions and room temperature resistance of 365 Ohm was used as a heater. It was glued to a sample end with a silver-filled epoxy. The resistive thermometers Cernox CX-1050-SD (Lake Shore Cryotronics, Inc.) were used for the temperature measurements. Thermometers were calibrated in the International Temperature Scale of 1990 (ITS-90). Indium-faces copper

clamps were used to attached the thermometers to a sample. The widths of contacts were 0.5–0.6 mm; the distance between two thermometers  $L_T$ , more correctly called as a mean separation between thermometer clamps, was about 27 mm (see Table II). Under steady conditions the temperature difference between thermometers was controlled to be small, 0.002–0.8 K. The thermal length  $L_{\text{th}}$ , that is the length over which the temperature gradient was established in a sample, was approximately by 4 mm smaller than the total length  $L$ . The thermal conductivity measurements were performed in the range from 2.4 to 420 K. A multi-layer radiation shield was mounted around the sample in order to reduce radiation heat loses from the heater and sample at temperatures above 300 K. Small corrections to measured data at these temperatures, which take into account the effect of remanent (residual) heat loses were applied. The uncertainty in the absolute value of thermal conductivity is estimated to be less than 2% over almost all temperature interval measured. The uncertainty in determination of thermometers separation contributes substantially to this error. At high temperatures, above approximately 300 K, an experimental error due to radiation heat loses increases very rapidly with temperature. We estimate that this experimental error is  $\lesssim 2\%$  at 420 K.

### III. RESULTS AND DISCUSSION

Experimental data on the temperature dependence of thermal conductivity of natural and enriched silicon crystals with [100] rod axis are shown in Fig. 1. Thermal conductivity for three samples of  $^{\text{nat}}\text{Si}$  have been measured. Two of them originate from the same parent crystal  $^{\text{nat}}\text{SiA}$  (see Table I), and have different orientation. All samples of  $^{\text{nat}}\text{Si}$  exhibit a very normal  $\kappa(T)$  dependence in over all temperature range studied. In Fig. 2, the comparison of our experimental data for silicon of natural isotopic composition with the reference data  $\kappa_{\text{ref}}(T)$  from Ref. [33] is shown. At low temperatures, where the  $\kappa(T)$  depends on the sample dimensions, the comparison is meaningless. At high temperatures, above 80 K, there is an overall good agreement between the data. However, the difference,  $\kappa(T)/\kappa_{\text{ref}}(T) - 1$ , shows anomaly at 150 K. Since our highly accurate and precise data demonstrate a quite smooth dependencies  $\kappa(T)$ , it appears that the reference data have a systematic error reaching 4% within temperature interval  $120 < T < 300$  K.

The maximum value of thermal conductivity over all samples is obtained for the most

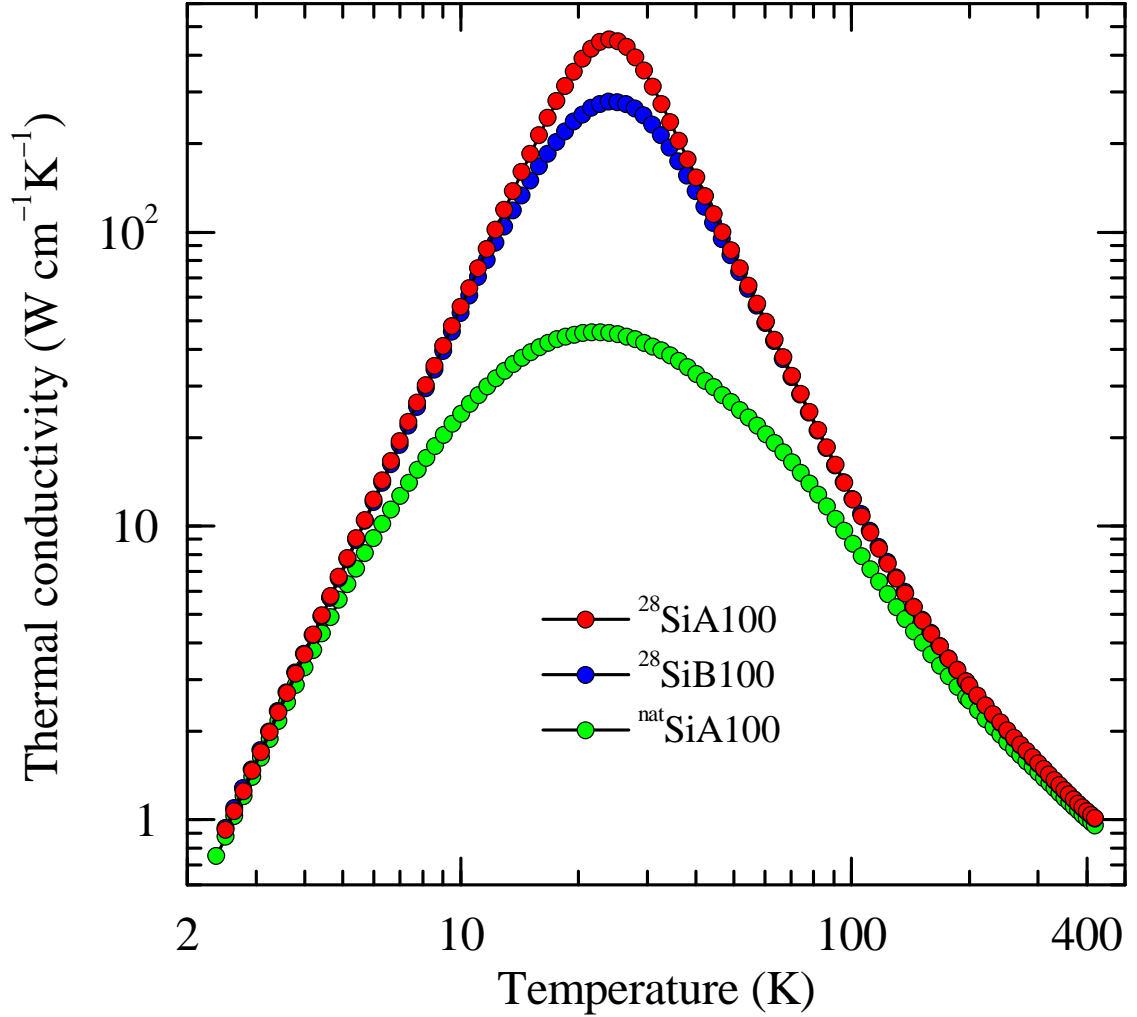


FIG. 1. Thermal conductivity of silicon single crystals along  $[100]$  axis as a function of temperature. Data for three crystals with different isotopic compositions are shown.

pure sample  $^{28}\text{SiA100}$ . It equals to  $450 \text{ W cm}^{-1}\text{K}^{-1}$  at  $24.1 \text{ K}$ . This value is the highest ever measured till now value for thermal conductivity of dielectrics at any temperature. The previous record,  $\kappa = 410 \text{ W cm}^{-1}\text{K}^{-1}$  at  $104 \text{ K}$ , was set for the isotopically pure single crystal diamond  $^{12}\text{C}(99.9\%)$  [5].

All enriched crystals show a symmetric, single and sharp peak in  $\kappa(T)$  at low temperatures (see Fig. 1). This peak shape is rather contrasting with calculated dependencies  $\kappa(T)$  which were obtained using generalized Callaway models that rely on the assumption that phonons of different polarizations independently contribute to the total conductivity [18, 19]. These calculated  $\kappa(T)$  demonstrate asymmetric and broad peaks arising from a large difference the phonon velocities for different polarizations. A similar result was obtained for germanium



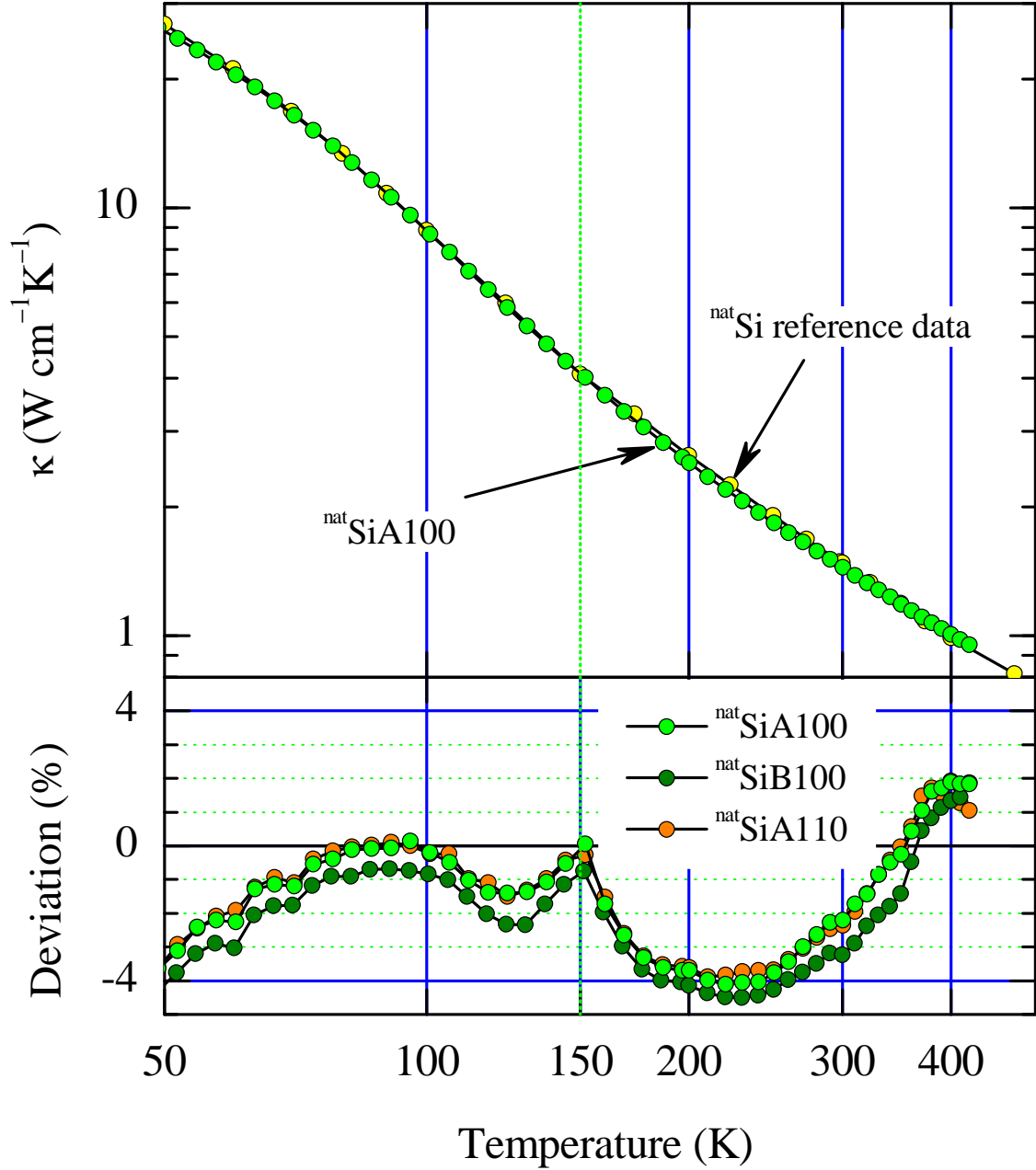


FIG. 2. Thermal conductivity as a function of temperature for silicon samples of natural isotopic composition. The lower panel: the relative difference between our data and the reference one [33].

in Ref. [8, 18].

In Fig. 3 the ratio of thermal conductivities of enriched crystals to that of <sup>nat</sup>SiB100 as a function of temperature is shown. At maximum the ratio attains 10, the temperature of the maximum is about 24 K. The isotope effect (for the crystal with the natural isotopic abundance) becomes almost zero at  $T < 2.5$  K. On the other hand the effect decreases

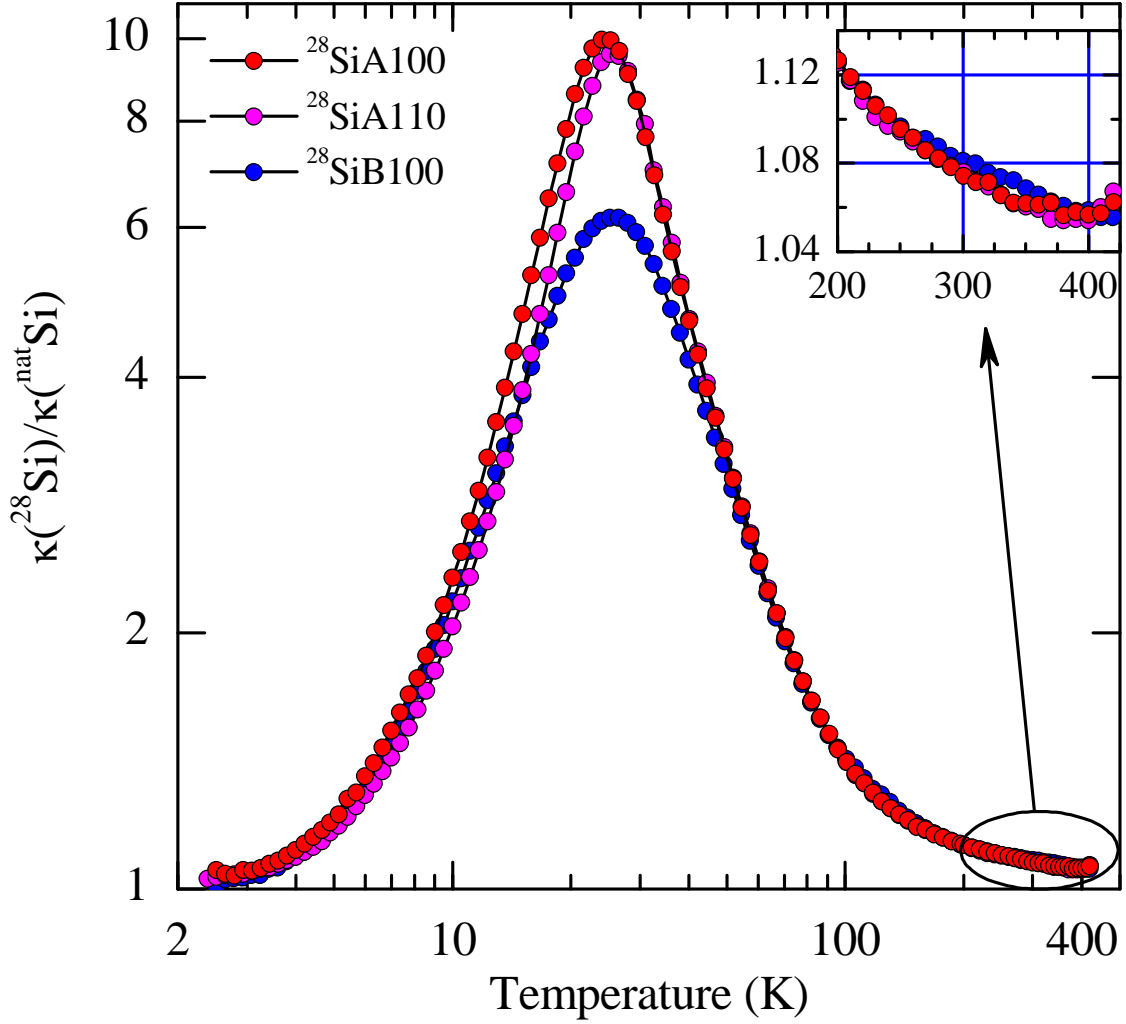


FIG. 3. The ratio of thermal conductivities of enriched crystals to that of  $^{\text{nat}}\text{SiB100}$  as a function of temperature.

at high temperatures being about  $8 \pm 1\%$  at 298 K (see insert in Fig. 3). This value is close to that (7–10%) found in Refs. [9–11]. At liquid nitrogen temperature (78 K) the isotope effect accounts 75%. From the Figs. 1 and 3 it is seen that dependencies  $\kappa(T)$  for  $^{28}\text{SiA}$  and  $^{28}\text{SiB}$  are the same within experimental errors at  $60 < T < 420$  K. This suggests that thermal conductivity of silicon does not depend upon the isotopic composition at concentration of isotope  $^{28}\text{Si}$  above 99.92%. That is the isotope scattering is much weaker than the phonon-phonon scattering. Below 60 K the isotope scattering contribution to the thermal conductivity in sample  $^{28}\text{SiB}$  increases sizably with decreasing temperature. At 40 K the thermal resistivity of  $^{28}\text{SiB}$  is about 12% higher than that of  $^{28}\text{SiA}$  due to this scattering. Since the isotope scattering rate for  $^{28}\text{SiB}$  is 16 times the rate for  $^{28}\text{SiA}$  (see

$g_2$  values in Table I), this scattering appears to be unimportant in thermal conductivity of  $^{28}\text{SiA}$  above about 40 K.

The  $\kappa(T)$  for the enriched crystals is very close to the cubic dependence at temperatures below 10 K that is expected for the regime of purely diffusive boundary scattering of phonons. Specifically we find that  $\kappa(T) \propto T^n$ , where  $n = 2.97 \pm 0.06$  for the purest sample  $^{28}\text{SiA}$ . The exponent  $n$  for  $^{\text{nat}}\text{Si}$  becomes equal to that for  $^{28}\text{SiA}$  below 2.5 K. Since the specific heat of silicon crystal follows the cubic temperature dependence below 9 K [34, 35], our low temperature data on  $\kappa(T)$  for the sample  $^{28}\text{SiA}$  suggest that the phonon mean free path reaches the maximum value determined only by the sample geometry and its orientation.

In Fig. 4 the dependencies of  $\kappa(T)$  for two pairs of samples with different orientations are shown. These data demonstrate the effect of phonon focusing on the thermal conductivity of silicon. At temperatures near and below the thermal conductivity maximum the  $\kappa(T)$  for samples with [100] orientations is higher than that for [110] samples. The phonon focusing effect is clearly seen for isotopically enriched silicon. This effect becomes sizable at  $T < 31$  K, and the ratio  $\kappa[100]/\kappa[110]$  stays nearly constant at 1.39 for temperatures below 14 K (the right-hand insert in Fig. 4). For  $^{\text{nat}}\text{Si}$  the phonon focusing is also observed below 31 K, the ratio  $\kappa[100]/\kappa[110]$  increases with decreasing of temperature down to  $\approx 3.5$  K; this ratio is about 1.38 at 3 K and smaller than the value 1.43 measured in Ref. [36]. According to the theory [37] the ratio  $\kappa[100]/\kappa[110] = 1.38$  for the silicon samples with square cross section and  $D/L = 0.1$ , and our values equal to this estimation within the experimental uncertainty. The 3D-plot of thermal conductivity for silicon rod with square cross-section as a function of orientation at fixed temperature in the boundary scattering regime is presented in left-hand insert in Fig. 4. These data were calculated using the theoretical approach developed in Ref. [38]. Above 31 K the conductivity is isotropic, as it must be for cubic crystals.

In Fig. 4 the experimental  $\kappa(T)$  for  $^{\text{nat}}\text{Si}$  rod with smaller cross-section and orientation [100] is shown ( $^{\text{nat}}\text{Si}100$ , Ref. [11]). As expected, it lies below the curve of its larger counterpart  $^{28}\text{SiA}100$  due to the higher rate of phonon boundary scattering in  $^{\text{nat}}\text{Si}100$ . The conductivity of  $^{\text{nat}}\text{Si}100$  is lower sizably than that of the larger rod even at temperatures up to 80–100 K, much higher than 31 K, at which the focusing effect die out. It appears that prerequisite of the phonon focusing effect in thermal conductivity is the long phonon mean free path comparable or exceeding cross-section dimensions of a sample, and the absence of phonon-phonon interactions.

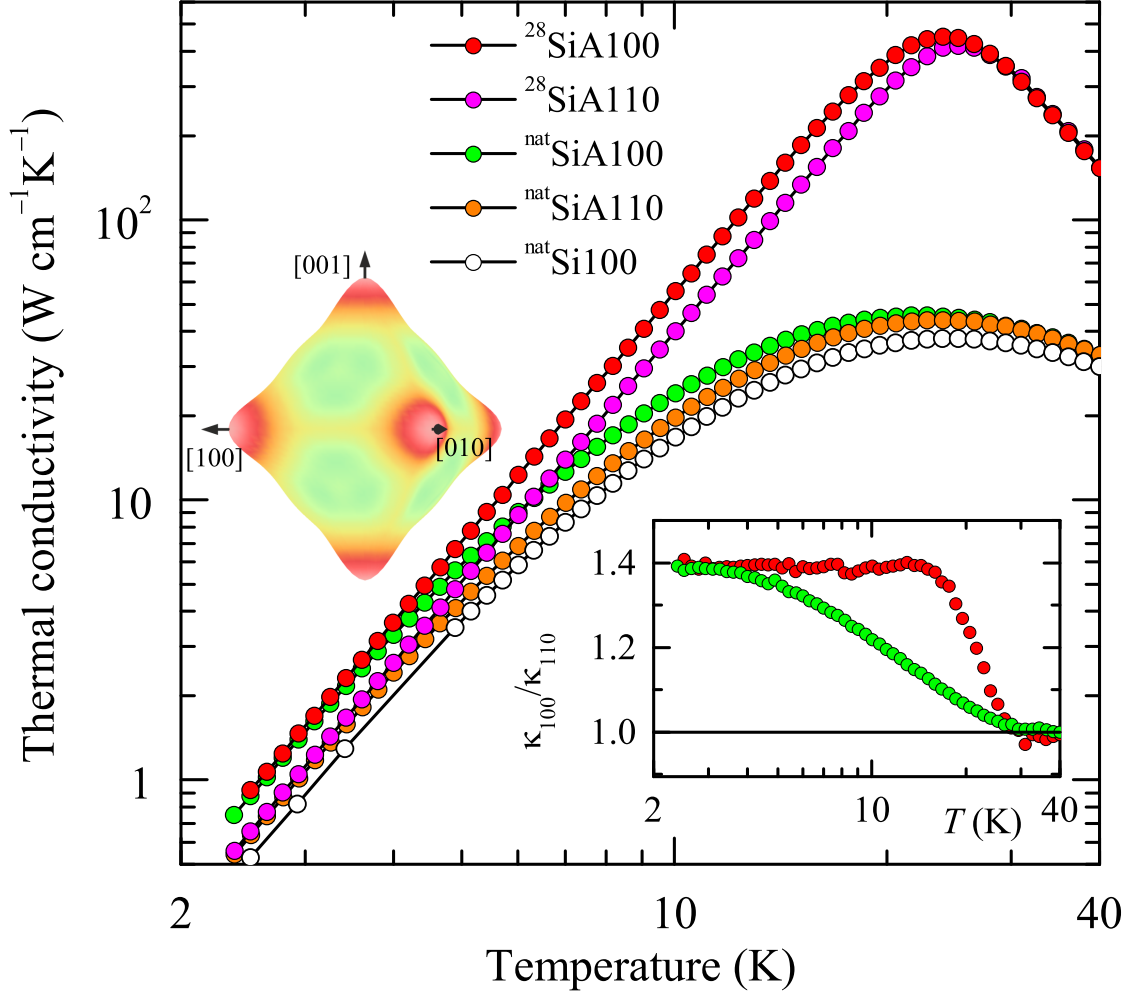


FIG. 4. The temperature dependencies of thermal conductivity for two pairs of samples with different orientations and isotopic compositions. Open circles denote the data from Ref. [11] for  $^{\text{nat}}\text{Si}$  oriented along [100] with small cross-section  $2.00 \times 3.12 \text{ mm}^2$ . The ratio of  $\kappa[100]/\kappa[110]$  as a function of temperature is shown in the right-hand insert. The left-hand insert shows the calculated orientation dependence of  $\kappa$  at fixed temperature in the boundary scattering regime.

#### IV. CONCLUSIONS

In summary, the thermal conductivity of three crystals of silicon with different isotopic composition has been measured accurately from 2.4 to 420 K. The isotope effect is  $8 \pm 1\%$  for silicon with natural isotopic composition at room temperature. Thermal conductivity of single isotope crystal containing 99.995% of  $^{28}\text{Si}$  reaches the maximum of  $450 \text{ W cm}^{-1}\text{K}^{-1}$  at 24 K, the highest value measured for dielectrics till now. This crystal shows nearly exact  $T^3$

dependence of  $\kappa(T)$  at temperatures below approximately 10 K. At temperatures near and below the conductivity maximum the thermal conductivity of silicon rod with orientation [100] is higher than that of the rod with orientation [110] due to the phonon focusing effect.

From the precise data obtained in this work it appears that the reference data values on  $\kappa(T)$  for single crystal silicon with natural isotopic composition near 150 K are inconsistent with the rest of the data within about 4% below 300 K. Our measured  $\kappa(T)$  for highly enriched silicon  $^{28}\text{Si}$  provides a most accurate approximation of the true temperature dependence of thermal conductivity of silicon governed solely by the intrinsic phonon-phonon scattering processes at temperatures from near the conductivity maximum to 420 K. The experimental data of this work, including the dependencies on isotope concentration and crystal orientation, provide a solid base for the verification of modern quantitative theories for the heat transport in dielectrics.

## ACKNOWLEDGMENTS

The authors thank A. M. Gibin, I. G. Keleyev, and I. I. Kuleyev for helpful discussion.

- 
- [1] E. E. Haller, Isotopically engineered semiconductors. *J. Appl. Phys.* **77**(7), 2857–2878 (1995).
  - [2] A. P. Zhernov and A. V. Inyushkin, Kinetic coefficients in isotopically disordered crystals. *Physics-Uspekhi* **45**(5), 527–552 (2002).
  - [3] T. R. Anthony, W. F. Banholzer, and J. F. Fleischer, L. Wei, P. K. Kuo, R. L. Thomas, and R. W. Pryor, Thermal diffusivity of isotopically enriched  $^{12}\text{C}$  diamond. *Phys. Rev. B* **42**(2), 1104–1111 (1990).
  - [4] J. R. Olson, R. O. Pohl, J. W. Vandersande, A. Zoltan, T. R. Anthony, W. F. Banholzer, Thermal conductivity of diamond between 170 and 1200 K and the isotope effect. *Phys. Rev. B* **47**, 14850–14856 (1993).
  - [5] L. Wei, P. K. Kuo, R. L. Thomas, T. R. Anthony, and W. F. Banholzer, Thermal conductivity of isotopically modified single crystal diamond. *Phys. Rev. Lett.* **70**(24), 3764–3767 (1993).
  - [6] A. A. Kaminskii, V. G. Ralchenko, H. Yoneda, A. P. Bolshakov, and A. V. Inyushkin, Stimulated Raman scattering-active isotopically pure  $^{12}$  and  $^{13}$  diamond crystals: A milestone in

- the development of diamond photonics. *JETP Lett.* **104**, 347 (2016) [*Pis'ma Zh. Eksp. Teor. Fiz.* **104**, 356 (2016)].
- [7] V. I. Ozhogin, A. V. Inyushkin, A. N. Taldenkov, A. V. Tikhomirov, G. E. Popov, E. Haller, and K. Itoh, Isotope effect in the thermal conductivity of germanium single crystals. *Pis'ma Zh. Eksp. Teor. Fiz.* **63**(6), 463–467 (1996) [*JETP Lett.* **63**(6), 490–494 (1996)].
- [8] M. Asen-Palmer, K. Bartkowski, E. Gmelin, M. Cardona, A. P. Zhernov, A. V. Inyushkin, A. N. Taldenkov, V. I. Ozhogin, K. M. Itoh, and E. E. Haller, Thermal conductivity of germanium crystals with different isotopic compositions. *Phys. Rev. B* **56**(15), 9431–9447 (1997).
- [9] A. V. Gusev, A. M. Gibin, O. N. Morozkin, V. A. Gavva, and A. V. Mitin, Thermal Conductivity of  $^{28}\text{Si}$  from 80 to 300 K. *Neorganicheskie Materialy* **38**(11), 1305–1307 (2002) [*Inorg. Mater.* **38**(11), 1100–1102 (2002)].
- [10] R. K. Kremer, K. Graf, M. Cardona, G. G. Devyatykh, A. V. Gusev, A. M. Gibin, A. V. Inyushkin, A. N. Taldenkov, and H.-J. Pohl, Thermal conductivity of isotopically enriched  $^{28}\text{Si}$ : revisited. *Solid State Commun.* **131**(8), 499–503 (2004).
- [11] A. V. Inyushkin, A. N. Taldenkov, A. M. Gibin, A. V. Gusev, and H.-J. Pohl. On the isotope effect in thermal conductivity of silicon. *Phys. Stat. Sol. C* **1**(11), 2995–2998 (2004).
- [12] A. V. Inyushkin, A. N. Taldenkov, A. Yu. Yakubovsky, A. V. Markov, L. Moreno-Garsia, and B. N. Sharonov, Thermal conductivity of isotopically enriched  $^{71}\text{GaAs}$  crystal. *Semicond. Sci. Technol.* **18**(7), 685–688 (2003).
- [13] P. G. Klemens, The scattering of low-frequency lattice waves by static imperfections. *Proc. Phys. Soc., London, Sec. A* **68**(12), 1113–1128 (1955).
- [14] P. Carruthers, Theory of thermal conductivity of solids at low temperatures. *Rev. Mod. Phys.* **33**(1), 92–138 (1961).
- [15] S. Tamura, Isotope scattering of dispersive phonons in Ge. *Phys. Rev. B* **27**(2), 858–866 (1983).
- [16] J. Callaway, Model for lattice thermal conductivity at low temperatures. *Phys. Rev.* **113**(4), 1046–1051 (1959).
- [17] R. Berman and J. C. F. Brock, The Effect of isotopes on lattice heat conduction. I. Lithium fluoride. *Proc. Roy. Soc., London, Ser. A* **289**, 46–65 (1965).
- [18] D. T. Morelli, J. P. Heremans, G. A. Slack, Estimation of the isotope effect on the lattice thermal conductivity of group IV and group III-V semiconductors. *Phys. Rev. B* **66**(19),

- 195304 (2002).
- [19] I. G. Kuleev and I. I. Kuleev, The effect of normal phonon-phonon scattering processes on the maximum thermal conductivity of isotopically pure silicon crystals. *Zh. Eksp. Teor. Fiz.* **122**(3), 558–569 (2002) [*JETP* **95**(3), 480–490 (2002)].
- [20] M. Omini and A. Sparavigna, Heat transport in dielectric solids with diamond structure. *Nuovo Cimento D* **19**(10), 1537–1563 (1997).
- [21] D. A. Broido, A. Ward, N. Mingo, Lattice thermal conductivity of silicon from empirical interatomic potentials. *Phys. Rev. B* **72**(1), 014308 (2005).
- [22] D. A. Broido, M. Malorny, G. Birner, Natalio Mingo, and D. A. Stewart, Intrinsic lattice thermal conductivity of semiconductors from first principles. *Appl. Phys. Lett.* **91**(23), 231922 (2007); doi:10.1063/1.2822891
- [23] A. Ward, D. A. Broido, D. A. Stewart, G. Deinzer, *Ab initio* theory of the lattice thermal conductivity in diamond. *Phys. Rev. B* **80**(12), 125203 (2009).
- [24] C. de Tomas, A. Cantarero, A. F. Lopeandia, and F. X. Alvarez, From kinetic to collective behavior in thermal transport on semiconductors and semiconductor nanostructures. *J. Appl. Phys.* **115**, 164314 (2014).
- [25] A. Jain, A. J. H. McGaughey, Effect of exchange-correlation on first-principles-driven lattice thermal conductivity predictions of crystalline silicon. *Comput. Mater. Sci.* **110** 115120 (2015).
- [26] I. G. Kuleyev, I. I. Kuleyev, and I. Yu. Arapova, Anharmonic processes of scattering and absorption of slow quasi-transverse modes in cubic crystals with positive and negative anisotropies of second-order elastic moduli. *J. Phys.: Condensed Matter* **20**(46), 465201 (2008).
- [27] K. Esfarjani, G. Chen, and H. T. Stokes, Heat transport in silicon from first-principles calculations. *Phys. Rev. B* **84**(2), 085294 (2011).
- [28] J. Ma, W. Li, and X. Luo, Examining the Callaway model for lattice thermal conductivity. *Phys. Rev. B* **90**, 035203 (2014).
- [29] P. Becker, H.-J. Pohl, H. Riemann, and N. Abrosimov, Enrichment of silicon for a better kilogram. *Phys. Status Solidi A* **207**(1), 49–66 (2010). DOI 10.1002/pssa.200925148
- [30] J. W. Ager, III, J. W. Beeman, W. L. Hansen, E. E. Haller, I. D. Sharp, C. Liao, A. Yang, M. L. W. Thewalt, and H. Riemann, High-purity, isotopically enriched bulk silicon. *J. Electrochem. Soc.* **152**(6), G448–G451 (2005). DOI 10.1149/1.1901674.

- [31] N. V. Abrosimov, D. G. Arefev, P. Becker, H. Bettin, A. D. Bulanov, M. F. Churbanov, S. V. Filimonov, V. A. Gavva, O. N. Godisov, A. V. Gusev, T. V. Kotereva, D. Nietzold, M. Peters, A. M. Potapov, H.-J. Pohl, A. Pramann, H. Riemann, P.-T. Scheel, R. Stosch, S. Wundrack, and S. Zakel, A new generation of 99.999% enriched  $^{28}\text{Si}$  single crystals for the determination of Avogadro constant, *Metrologia* **54** (2017) 599609.
- [32] H. Lundt, M. Kerstan, A. Huber, P. O. Hahn, Subsurface damage of abraded silicon wafers. In: *Proceedings of 7th international symposium on silicon materials science and technology*. The Electrochemical Society, Pennington, NJ, Vol. 94-10, pp. 218–224 (1994).
- [33] C. Y. Ho, R. W. Powell, and P. E. Liley, Thermal conductivity of the elements. *J. Phys. Chem. Ref. Data* **1**, 279–425 (1972).
- [34] P. Flubacher, A. J. Leadbetter, J. A. Morrison, The heat capacity of pure silicon and germanium and properties of their vibrational frequency spectra. *Philos. Mag.* **4**(39), 273–294 (1959).
- [35] A. Gibin, G. G. Devyatykh, A. V. Gusev, R. K. Kremer, M. Cardona, H.-J. Pohl, Heat capacity of isotopically enriched  $^{28}\text{Si}$ ,  $^{29}\text{Si}$  and  $^{30}\text{Si}$  in the temperature range  $4\text{ K} < T < 100\text{ K}$ . *Solid State Commun.* **133**, 569–572 (2005).
- [36] A. K. McCurdy, H. J. Maris, and C. Elbaum, Anisotropic heat conduction in cubic crystals in the boundary scattering regime. *Phys. Rev. B* **2**(10), 4077–4083 (1970).
- [37] A. K. McCurdy, Phonon conduction in elastically anisotropic cubic crystals. *Phys. Rev. B* **26**(12), 6971–6986 (1982).
- [38] I. I. Kuleev, I. G. Kuleev, S. M. Bakharev, A. V. Inyushkin, Features of phonon transport in silicon rods and thin plates in the boundary scattering regime. The effect of phonon focusing at low temperatures. *Physica B* **416**, 81-87 (2013). <http://dx.doi.org/10.1016/j.physb.2013.02.020>